**Available online at www.ejournals.uofk.edu**

**Proceedings Vol. 6 pp. 124-131**
7th Annual Conference for Postgraduate Studies and Scientific Research
Basic Sciences and Engineering Studies - University of Khartoum
Theme: Scientific Research and Innovation for Sustainable Development in Africa
20-23 February 2016, Friendship Hall, Khartoum, Sudan

# Interaction mechanism for energy transfer in Ce,Tb co-doped LaF3

**H. A. A. Seedahmed[1],Ntwaeaborwa[2] and R.E. Kroon[2]**

[a]*Department of Physics, Faculty of Education, University of Khartoum, Omdurman, Sudan*

[b]*Department of Physics, University of the Free State, Bloemfontein, South Africa*

Abstract:$LaF_3$ pure host, $LaF_3$:Ce, $LaF_3$:Tb as well as $LaF_3$:Ce,Tb phosphors were synthesized by the hydrothermal method. X-ray diffraction measurements are in good agreement with the standard data of $LaF_3$ from JCPDS card 32-0483 and indicate that the material is nanocrystalline with a particle size of about 36 nm. Photoluminescence spectra of co-doped samples revealed that the $Ce^{3+}$ emission is quenched, while an enhancement of $Tb^{3+}$ emission occurred, implying an energy transfer from $Ce^{3+}$ (the donor) to $Tb^{3+}$ (the acceptor) in this system. MATLAB was used to fit the luminescence intensities and lifetimes of the donor for different concentrations of acceptor to theoretical models in order to investigate the energy transfer mechanism. The experimental data fitted the theoretical curves corresponding to the quadrupole-quadrupole and exchange interactions well. The effective average Bohr radius from the fit to the exchange model is around 1 Å. Since this is close to the ionic radius of the $Ce^{3+}$ and $Tb^{3+}$ ions, it suggests that the exchange interaction may contribute to the energy transfer mechanism.

**Keywords:***Energy transfer, Lanthanum fluoride, Cerium, Terbium, Interaction mechanism*

## INTRODUCTION

Developing the efficiency of luminescence materials has attracted much interest in the last five decadesdue to their wide application in modern technologies. One way to enhance the luminescence efficiency is through energy transfer between a donor and an acceptor. Among lanthanide ions, $Ce^{3+}$is an ideal donor candidate due to its allowed f-d absorption and its broad emission bandwhich can overlap the acceptor absorption band. The bright green emission of $Tb^{3+}$makes this ion a popular acceptor ofthe lanthanide group. Lanthanum fluoride is considered to be an ideal host material for luminescent lanthanide ions [1,2]. Because of the low-energy phonons (~350 $cm^{-1}$) of $LaF_3$ [1], quenching of the excited states of the guest lanthanide ions is minimal[1].The hydrothermal method is favourable for preparing $LaF_3$using precursors soluble in water like $La(NO_3)_3$ and NaF since $LaF_3$ is insoluble in water and $LaF_3$ precipitations can easily be obtained by centrifuging.Ce and Tb doped $LaF_3$and energy transfer from Ce to Tb in $LaF_3$has been reported [2-11].In this study, the mechanism responsiblefor the energy transfer between Ce and Tb was investigated by fitting the luminescence intensity and the lifetime of the donor as a function of acceptor concentration to the Inokuti and Hirayama [12] theoretical models.

## EXPERIMENTAL

$LaF_3$ pure host, $LaF_3$:Ce, $LaF_3$:Tb as well as $LaF_3$:Ce,Tb phosphor were synthesized by the hydrothermal method. $La(NO_3)_3.6H_2O$ and NaF were used as starting materials and $Ce(NO_3)_3.6H_2O$ and $Tb(NO_3)_3.6H_2O$were added fordoping. Cetyltrimethylammonium bromide $C_{19}H_{42}BrN$(CTAB) served as a surfactant to control the particle size.Each prepared sample contained 5mmol of the lanthanide ions (including dopant), 15 mmol of NaF and 1 mmol of CTAB.The nitrates, dissolved in 30 ml of water, were added to the CTAB in10 ml water.After stirringfor 20 min,NaF dissolved in 10 ml of water wasadded drop by drop. After further stirring for 40 min, the mixturewas transferred into a 125 ml autoclavelined with teflonand heated at 150°Cfor 12 h. The product was collected by centrifugation and washedfirst with water, and then with ethanol, each three times.The powder wasfinally dried in an oven at 80°C. By repeated dilution of a terbium nitrate solution, a series of $LaF_3$:Ce(1mol%),Tb(x mol%) where x = 20, 10, 5, 2, 1, 0.5, 0.2, 0.1, 0.05 was prepared.

The structure of the prepared samples wascharacterised by X-ray diffraction (XRD) with a Bruker D8 diffractometer. Auger spectra and scanning electron microscopy (SEM) images were collected with a PHI 700 Scanning Auger Nanoprobe. Photoluminescence (PL) spectra were obtained witha Cary

Eclipse fluorescence spectrophotometer. The luminescence decay curves were recordedat the SUPERLUMI station with synchrotron radiation at HASYLAB, DESY.

## THEORETICAL CONSIDERATIONS

The non-radiative transfer of an electronic excitation from a donor to an acceptor can be represented by

$$D^* + A \rightarrow D + A^* \quad (1)$$

where$D$represents the ground state of the donor and $A$ the ground state of the acceptor, and $D^*$ and $A^*$ represent their excited states. It has been shown that the transfer rate between the initial and final states is given by [13]

$$W_{DA} = \frac{2\pi}{\hbar}|\langle DA^*|\mathcal{H}_{DA}|D^*A\rangle|^2 \int f_D(E) f_A(E) dE \quad (2)$$

where$\langle DA^*|$ is the final state, $|D^*A\rangle$ is the initial state and $\mathcal{H}_{DA}$ is the interaction Hamiltonian. The integral represent the spectral overlap between the donor ($D$) emission spectrum and the acceptor ($A$) absorption spectrum. The normalised emission spectrum of the donor is $f_D(E)$ and the normalised absorption spectrum of the acceptor is $f_A(E)$. The mechanism for energy transfer depends on the interaction Hamiltonian.

If the wavefunctions of the donor and acceptor overlap, the quantum mechanical exchange interaction results in a transfer rate [14]

$$W_{DA} = \frac{1}{\tau_0}\exp\left(\frac{2R_0}{L}\left[1-\frac{r}{R_0}\right]\right) \quad (3)$$

where $\tau_0$ is the donor lifetime in the absence of the acceptor, $r$is the distance between donor and acceptor, $R_0$ is the so-called critical separation distance for which energy is transferred at the same rate as which it decreases via luminescence when no acceptors are present, and $L$ is a scaling factor corresponding to an effective Bohr radius. The corresponding decay function $\phi(t)$after pulse excitation is given by [12]

$$\phi(t) = \exp\left[\frac{-t}{\tau_0} - \gamma^{-3}\frac{c}{c_0}\mathrm{g}\left(\frac{t}{\tau_0}e^{\gamma}\right)\right] \quad (4)$$

where the exchange constant $\gamma$ is related to the scaling factor $L$ by $\gamma = 2R_0/L$ and $\mathrm{g}\left(\frac{t}{\tau_0}e^{\gamma}\right)$ is a function that can be evaluated numerically [12], while $c$ is the acceptor concentration and $c_0$ is the critical concentration related to the critical radius by

$$c_0 = 3/(4\pi R_0^3). \quad (5)$$

For larger separation distances non-radiative energy transfer may occur via electric multipole interactions, resulting in an energy transfer rate [15]

$$W_{DA} = \frac{1}{\tau_0}\left(\frac{R_0}{r}\right)^s \quad (6)$$

where$s$ = 6 for dipole-dipole, 8 for dipole-quadrupole and 10 for quadrupole-quadrupole interactions. The corresponding decay function is [12]

$$\phi(t) = \exp\left[\frac{-t}{\tau_0} - \Gamma\left(1-\frac{3}{s}\right)\frac{c}{c_0}\left(\frac{t}{\tau_0}\right)^{3/s}\right]. \quad (7)$$

As a result of energy transfer, the luminescence intensity as well as the lifetime of the donor decreases. Inokuti and Hirayama [8] developed numerical methods to simulate these changes for the different interactions mechanisms. The relative emission intensity of the donor can be calculated from

$$\frac{I}{I_0} = \frac{1}{\tau_0}\int_0^{\infty}\phi(t)dt \quad (5)$$

where$I$ is the donor emission intensity in the presence of the acceptor, and $I_0$the corresponding intensity in the absence of acceptors. Similarly, the mean decay time $\tau_m$ can be calculated from

$$\tau_m = \int_0^{\infty} t\phi(t)dt \Big/ \int_0^{\infty}\phi(t)dt. \quad (6)$$

MATLAB was used to calculate the theoretical decay functions $\phi(t)$ as well as the relative emission intensities $\frac{I}{I_0}$ and the reduced mean decay times $\frac{\tau_m}{\tau_0}$ as a function of the concentration $c/c_0$ for the different energy transfer mechanisms in order to compare these theoretical results to experimental data.

## RESULTS AND DISCUSSION

Figure 1 shows the XRD patterns of undoped and doped $LaF_3$, together with the standard data for $LaF_3$ from JCPDS card 32-0483. The patterns for samples doped with 5 mol% of either Ce or Tb have almost no difference from the pure host, showing that the Ce and Tb ions were incorporatedsuccessfully and were well dispersed in the $LaF_3$lattice. The heavily doped $LaF_3$:Ce(1%),Tb(20%) sampleshows a slight shift in the diffraction peaks toward greaterangles,implyingthat the lattice parameter has decreased, which is reasonable in terms of the smaller Tb ionic radius (0.923Å) compared to the La ions (1.061 Å) that are substituted [6].

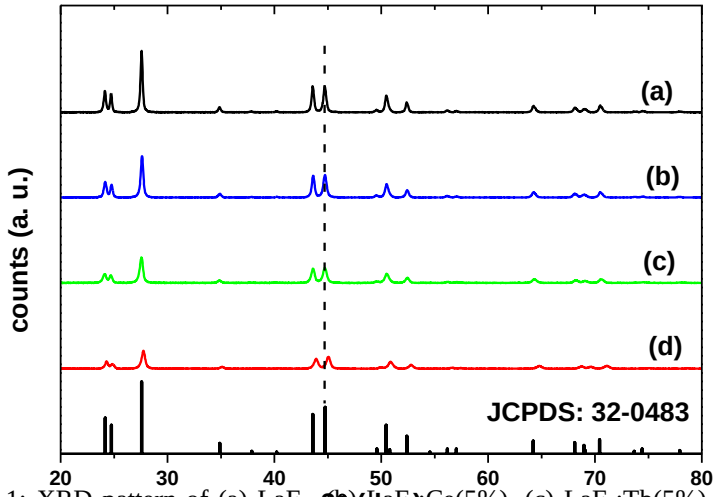


Fig. 1: XRD pattern of (a) $LaF_3$, (b) $LaF_3$:Ce(5%), (c) $LaF_3$:Tb(5%), and (d) $LaF_3$:Ce(1%)Tb(20%). The bottom vertical lines are the standard data of $LaF_3$ from JCPDS card 32-0483.

The particle size $\tau$was estimated from the Scherrer equation [16]

$$\tau = \frac{K\lambda}{\beta \cos\theta} \quad (1)$$

where$K$ is the shape factor(0.9), $\lambda$ is the wavelength, $\beta$ is the FWHM(corrected for the instrument response) of the x-ray peak at the Bragg angle$\theta$. The average particle size of the $LaF_3$was 36 nm. For the doped samples the peaks are slightly wider than the undoped sample, but this can be explained by impurity broadening instead of a decrease in particle size.

Figure 2 presentsa SEM image and Auger profile of pure $LaF_3$. Charging on the insulating samples prevented better resolution images, so the particle shape is not clear,but it can be seen that the particle size is less than 50 nm. The Auger peaks at 83, 528, 634 and 732 eV are associated with the La while the peak at 659 eV corresponds to F. The peak at 273 eVis associated with C. The C contamination is attributed to adventitious hydrocarbons which areknown to be always present.

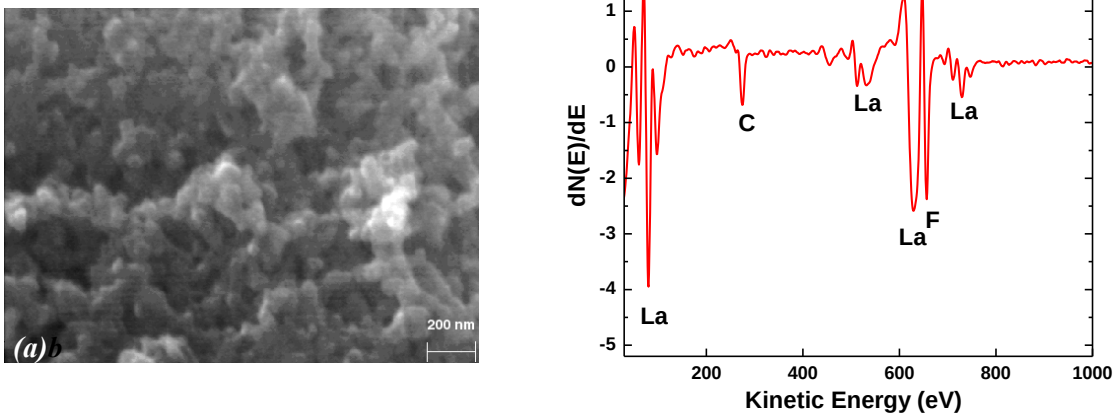


Fig. 2:(a) SEM image and (b) Auger spectrum of pure $LaF_3$

Figure 3 shows the PL excitation and emission forthe $LaF_3$:Ce(1%) measured at room temperature. The excitation spectrum has a broad peak with a maxima at 247 nm corresponding to the 4f-5d absorption band of the $Ce^{3+}$ ions. The broad emission spectrum exhibit two peaks centred at 287 and 301 nm attributed to the transitions from the lowest 5d excited state to the 4f ($^2F_{7/2}$ and $^2F_{5/2}$) ground state. Both the excitation and emission spectra are inagreement with the reported data [3].

Excitation and emission spectra for $LaF_3$:Tb(5%) sample are shown in Figure 4. The excitation spectrum was recorded using the 542 nm green emission of $Tb^{3+}$ ions. Nine absorption bands have beenidentified to correspond to f-f transitions of $Tb^{3+}$ from the $^7F_6$ ground stateto $^5I_7$ at 272 nm, $^5I_8$,$^5F_5$at 284 nm, $^5H_6$ at 303 nm, $^5H_7$ at 318 nm, $^5D_1$ at 326 nm, $^5L_8$ at 342nm, $^5D_2$,$^5L_9$at 352 nm, $^5L_{10}$ at 370 nm and $^5D_3$,$^5G_6$at 379 nm[17]. Although Wang *et al.* [8]states that 4f-5d absorption bands of $Tb^{3+}$ ions in $LaF_3$occur from 250–280 nm, the lowest energy f-d absorption actually occurs near 200 nm[18]. The absorption band at 247 nm does not appear to be due to f-f or f-d absorption of $Tb^{3+}$ and is most likely caused by very small amounts of $Ce^{3+}$ impurity (note that the wavelength matches the f-d absorption of Ce in Figure 3) which could come from the porous teflon liner used for sample preparation with other samples containing Ce.

The emission spectrum obtained from the Tb doped samples by exciting with 352 nm showed the characteristic green emission bands attributed to the $^5D_4$-$^7F_J$ transitions (J=6,5,4,3)of $Tb^{3+}$, with the dominant green band at 542 nm.

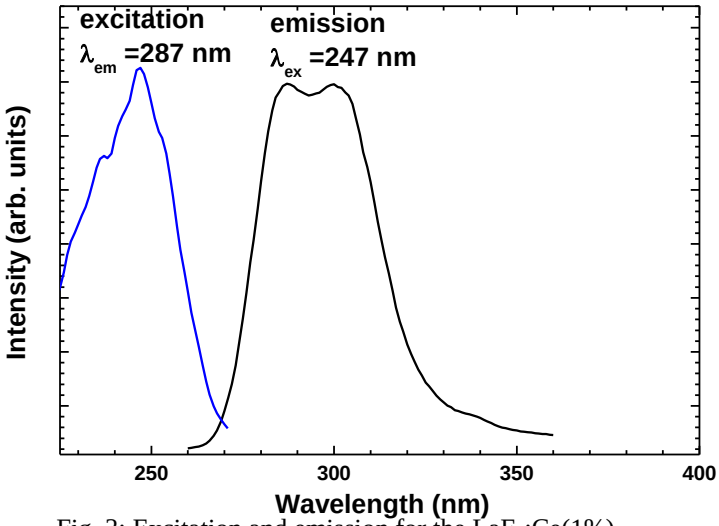


Fig. 3: Excitation and emission for the $LaF_3$:Ce(1%)

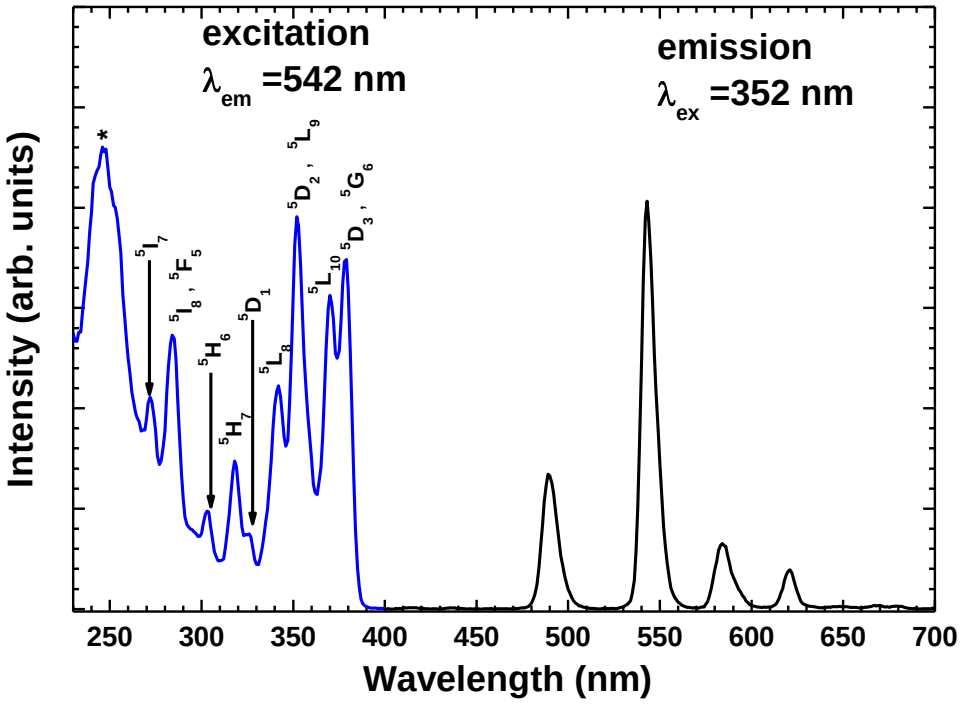


Fig. 4: Excitation and emission spectra for $LaF_3$:Tb(5%). Label for f-f transition are from $^7F_6$ ground state. The absorption peak marked with ($^*$) is attributed to small amounts of Ce impurity.

Figure 5 shows the PL emission spectrum of the $LaF_3$:Ce(1%),Tb(5%)co-doped sample excited at 247 nm, compared to the emission spectra for the singly doped samples.The Ce emission in the co-doped sample was quenched and an enhancement of the Tb emission was observed. This can be attributed to energy transfer from the $Ce^{3+}$ ions to $Tb^{3+}$ ions. Figure 6 shows the overlap of the emission spectrum of $LaF_3$:Ce(1%) and the excitation spectrum of $LaF_3$:Tb(5%). The Ce emission overlaps several of the Tb f-f excitation bandswhich isthe essentialcondition for energy transfer to occur

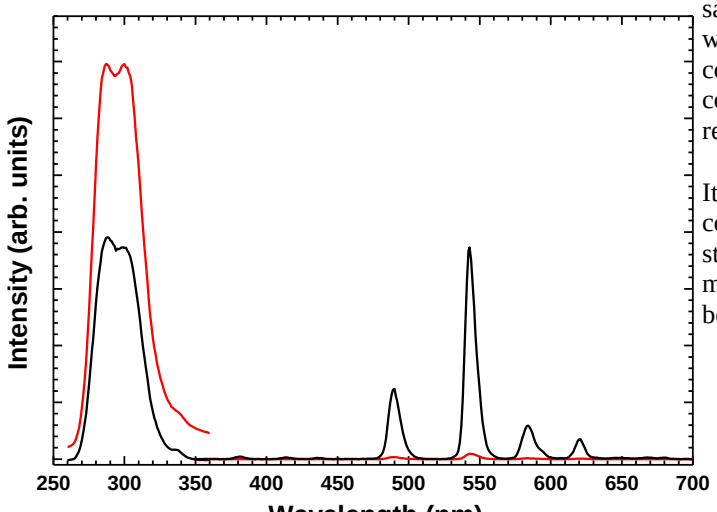


Fig. 5: PL spectrum of the $LaF_3$:Ce(1%),Tb(5%) sample excited with 247 nm (black) comparing with the PL of $LaF_3$:Ce(1%) and $LaF_3$:Tb(5%) samples (red)

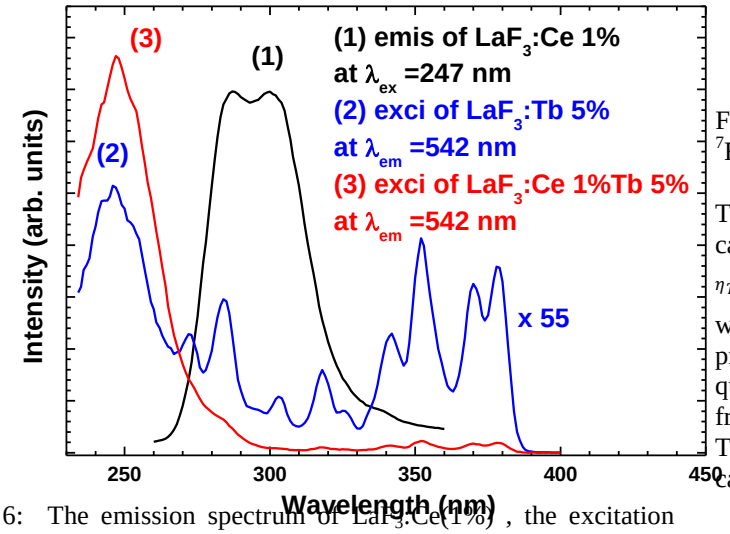


Fig. 6: The emission spectrum of $LaF_3$:Ce(1%) , the excitation spectrum of $LaF_3$:Tb(5%), and the excitation spectrum of $LaF_3$:Ce(1%),Tb(5%)

To investigate the influence of the Ce concentration on the emission intensity from Tb in the co-doped samples, the concentration of $Tb^{3+}$ ions was kept constant at 5 mol% and the concentration of $Ce^{3+}$ ions was varied from 0 up to 5 mol%. Figure 7 shows the relative intensity of Tb emission associated with the $^5D_4$-$^7F_5$ transition near 542 nm as a function of Ce concentration, normalized with respect to the sample containing no Ce, i.e. the Tb single doped sample. It was found that the Tb emission increased as the Ce concentration increased up to 5 mol%. Although the concentration of Ce corresponding to a maximum was not reached, the rate of increase became relatively low.

It was decided to study the transfer mechanism using a Ce concentration of 1 mol%, as a compromise between obtaining strong Tb emission through energy transfer but not introducing more Ce than was necessary to avoid any possible interaction between Ce-Ce ions which may occur at high concentration.

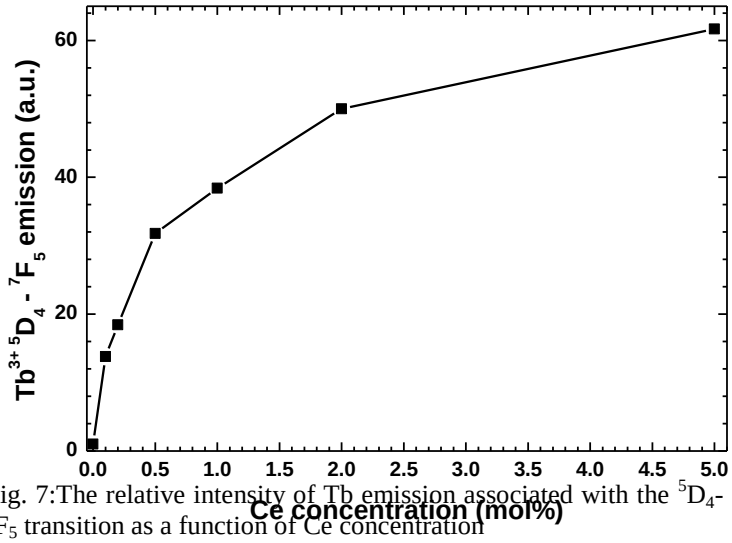


Fig. 7:The relative intensity of Tb emission associated with the $^5D_4$-$^7F_5$ transition as a function of Ce concentration

The quantum efficiency of the energy transfer $\eta_T$can be calculated by [19]

$$\eta_T = 1 - \frac{I_D}{I_{D0}} \qquad (2)$$

where$I_{D0}$ and $I_D$ are the PL intensity of Ce in the absence and presence of Tb with the same Ce concentration. The maximum quantum efficiency of the energy transfer achieved was 87% from $LaF_3$:Ce(1%),Tb(20%).

The quantum efficiency of the energy transfer $\eta_T$can be calculated by [19]

$$\eta_T = 1 - \frac{I_D}{I_{D0}} \qquad (2)$$

where$I_{D0}$ and $I_D$ are the PL intensity of Ce in the absence and presence of Tb with the same Ce concentration. The maximum quantum efficiency of the energy transfer achieved was 87% from $LaF_3$:Ce(1%),Tb(20%).

The luminescence intensity and decay lifetime of the donor as a function of the acceptor concentration was studied to determine the mechanism of the energy transfer between the Ce and the Tb ions in LaF3.

Values of I/I_0 for a fixed Ce donor concentration of 1 mol% and a range of Tb acceptor concentrations were measured with the Cary-Eclipse fluorescence spectrophotometer and the results are given in Figure 8 and Table 1.

The Ce donor lifetime curves were measured using synchrotron radiation at SUPERLUMI using photon counting with a photomultiplier tube detector, with an excitation wavelength of 247 nm. The time between bunches limited the measuring period to about 70 ns. The experimental curves were fitted (using the linear least squares routine in MATLAB) to multi-exponential functions (3 exponentials were found to be adequate) which were convoluted with the stray light signal measured on the system, and the fitted multi-exponential curves were used to calculate the mean decay times τ_m. The decay curve for singly doped LaF:Ce 1 mol% was processed in the same way as for the co-doped samples but with only a single-exponential function, and the lifetime was found to be 29 ns for the 287 nm emission and 31 ns for the 301 nm emission. The decay time was slightly longer for the longer wavelength emission, as also reported for Ce doped NaCaPO4 [20].

Figure 9 presents several of the processed lifetime decay curves. The blue curve is the measured data and the red points are the convolution of the fitted data.

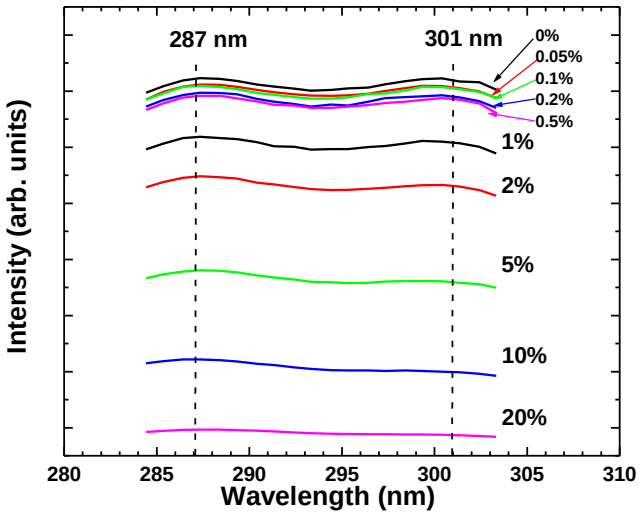


Fig. 8:The intensity of Ce emission for a range (0%-20%) of Tb concentration

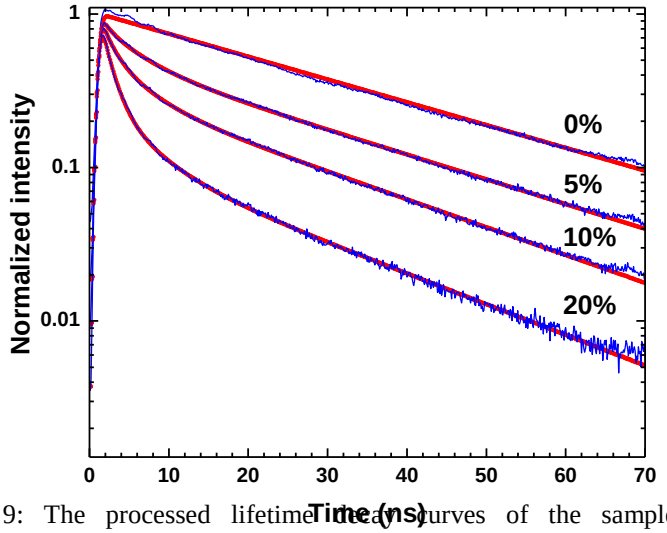


Fig. 9: The processed lifetime decay curves of the samples $LaF_3$:Ce(1%),Tb(x%) where x is 0%, 5%, 10%, and 20%. The blue curve is the measured data and the red points are the convolution of the fitted data.

Table 1 Luminescence intensity and lifetime for the $LaF_3$:Ce,Tb

| Acceptor concentration (mol%) | $\frac{I}{I_0}$ | $\tau_m$ (ns) | $\frac{\tau_m}{\tau_0}$ |
|---|---|---|---|
| 0 | 1 | 29.23 | 1 |
| 0.0500 | 0.984 | 28.63 | 0.979 |
| 0.100 | 0.981 | 28.58 | 0.978 |
| 0.200 | 0.964 | 28.50 | 0.975 |
| 0.500 | 0.956 | 28.25 | 0.966 |
| 1.00 | 0.855 | 27.87 | 0.954 |
| 2.00 | 0.758 | 27.62 | 0.945 |
| 5.00 | 0.526 | 24.24 | 0.829 |
| 10.0 | 0.306 | 19.79 | 0.677 |
| 20.0 | 0.134 | 14.09 | 0.482 |

Figure 10 (a) shows the experimental data $I/I_0$ and $\tau_m/\tau_0$associated with the peak at 287 nm (closed shape) plotted against one another and compared to the theoretical curves expected for different types of multipole interactions, which were calculated using the method of Inokuti and Hirayama [12]. The results match what one may expect if the energy transfer occurs due to quadrupole-quadrupole interaction, and is not consistent with either dipole-dipole or dipole-quadrupole interactions.To determine the critical concentration $c_0$, least squares fits were made for the quadrupole-quadrupole interaction of $I/I_0$against $c/c_0$and $\tau_m/\tau_0$against $c/c_0$ with $c_0$ as the fit parameter, giving values of 8.58 and9.77 mol% respectively. These wereaveragedand the result was converted to a volume concentration (using a molar volume of 33 $cm^3$/mol for $LaF_3$) and used to calculate the critical distance $R_0$of 5.2Å.

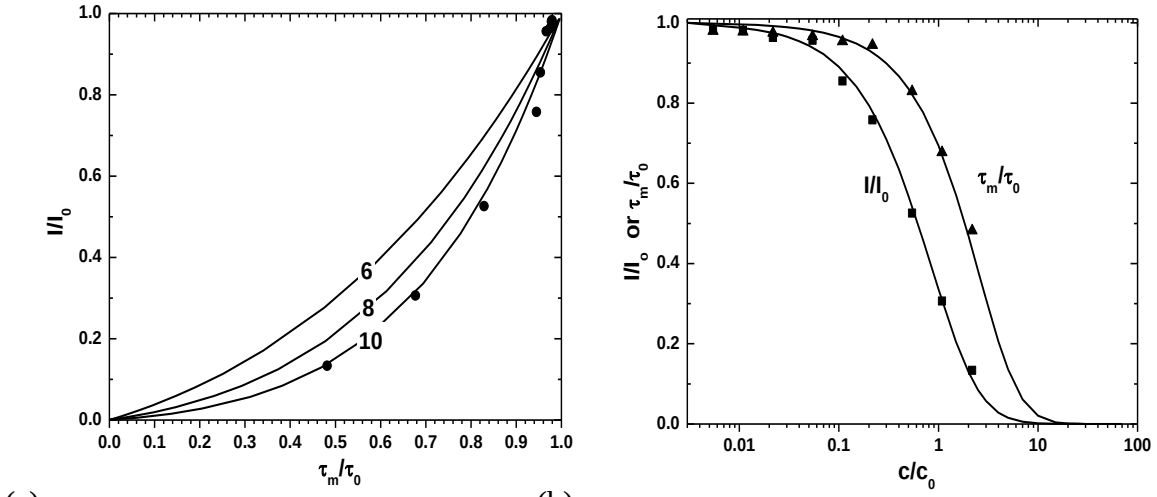


(a) (b)

Fig.10:(a) Experimental data of $\frac{I}{I_0}$ vs $\frac{\tau_m}{\tau_0}$ (closed circle) fitted to the theoretical curves (solid lines) of dipole-dipole (s=6), dipole-quadrupole (s=8), and quadrupole-quadrupole (s=10) interaction. (b) Experimental data of $\frac{I}{I_0}$(closed square) vs $\frac{c}{c_0}$and$\frac{\tau_m}{\tau_0}$ (closed triangle)vs $\frac{c}{c_0}$ fitted to the theoretical curves (solid lines) of quadrupole-quadrupole interaction.

The experimental data was also fitted to the exchange interaction model for energy transfer. For this model, in addition to$c_0$, the exchange constant $\gamma$ is also a parameter. The experimental data of $I/I_0$ and $\tau_m/\tau_0$were plotted against one another and compared to the theoretical curves of several values of $\gamma$as computed using the method of Inokuti and Hirayama [12]. The experimental data corresponds well to the exchange interaction for $\gamma$ =11.6 (see Figure 11(a)). This value for$\gamma$was fixed and least squares fits of $I/I_0$ against $c/c_0$ and $\tau_m/\tau_0$against $c/c_0$ with $c_0$ as the fit parameterwere made for exchange model in order to determine the critical concentration $c_0$ giving values of8.02 and 7.97 mol% respectively. The average critical concentration was used to calculate the critical distance$R_0$of 5.5 Å. The effective average Bohr radius $L$related to these values of $R_0$and $\gamma$ is 0.95 Å. This means the exchange interaction mechanism may contribute the energy transfer between Ce and Tb.

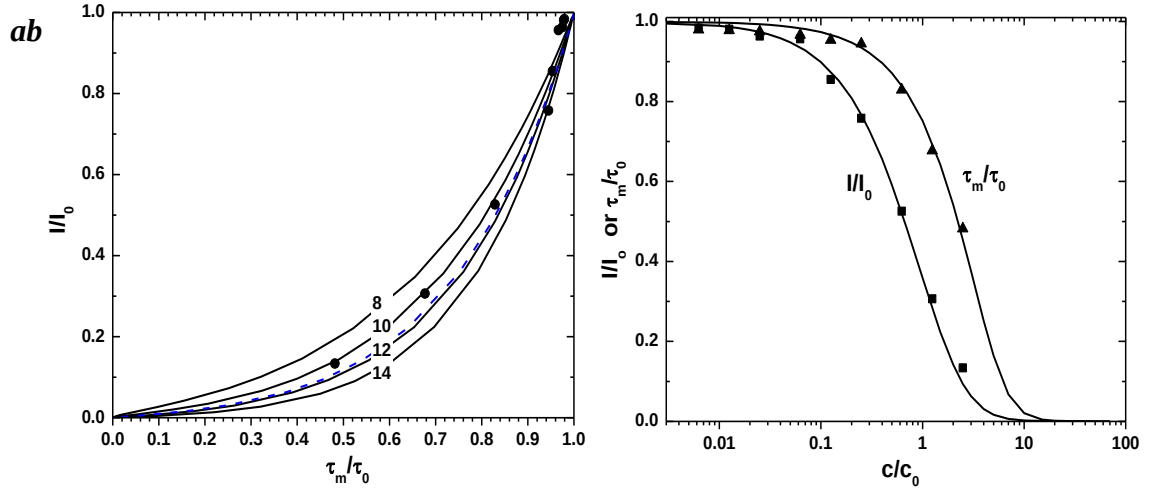


Figure 11(a) Experimental data of $\frac{I}{I_0}$ vs $\frac{\tau_m}{\tau_0}$(closed circle) fitted to the theoretical curves (solid lines) of exchange interaction ($\gamma$ = 8, 10, 12 and 14). The blue dashed line gives the best fit ($\gamma$ = 11.6).(b) Experimental data of $\frac{I}{I_0}$(closed square) vs $\frac{c}{c_0}$and $\frac{\tau_m}{\tau_0}$ (closed triangle) vs $\frac{c}{c_0}$ fitted to the theoretical curves (solid lines) of exchange interaction

The mechanism response of energy transfer from Ce to Tb in hostsother than $LaF_3$ has been reported by several authors. Wang *et al.* [21] found the dipole-dipole interaction for $CaAl_2SiO_6$ hostwhile Cao *et al.* [22] reported the dipole-quadrupole mechanism for $Mg_{1-x}Mn_xAl_{11}O_{19}$ host. To our knowledge no one has reported the quarupole-quadrupole interaction between Ce and Tb before, although it has been found for Eu and Pr in $K_5Li_2GdF_{10}$ host[23]. With this high acceptor concentration (up to 20 mol%) in our system, the critical distance $R_0$ becomesvery short,making it possiblethat the quadrupole-quadrupole interaction as well as the exchange interaction occur.According to Nakazawa and Shionoya [24] it is very difficult to distinguish between the dipole-quadrupole, quadrupole-quadrupole and exchange interactions by analysing the luminescence intensity and lifetime of the donor emission.

## CONCLUSION

Ce and Tb have been successfully incorporated singly as well as together in $LaF_3$via the hydrothermal method. The crystal structure of $LaF_3$ remained unchanged after being doped with $Ce^{3+}$ and $Tb^{3+}$ ions, with a slight decrease in the lattice parameter in the samples having a heavy dopant concentration. The estimated particle size was 36 nm.

The excitation and emission spectra of the single doped samples are in a good agreement with the reported values. Energy transfer from Ce to Tb was achieved in the co-doped samples with maximum quantum efficiency for energy transfer around 87% for the $LaF_3$:Ce(1%),Tb(20%) sample.

The data associated with the luminescence intensity and lifetime of the donor as a function of the acceptor concentration fitted well to the Inokuti and Hirayama nonradiative energy transfer models corresponding to the quadrupole-quadrupole mechanism and the exchange interaction mechanism. Due to the short effective average Bohr radius *L* calculated from the obtained fitted parameters, the exchange interaction could not be excluded and it may contribute to the energy transfer together with quadrupole-quadrupole interaction.

## REFERENCES

[1] Zhang X, Hayakawa T and Nogami M 2011 *Int. J. Appl. Ceram. Technol.***8** 741

[2] Li C, Liu X, Yang P, Zhang C,Lian H and Lin J 2008 *J. Phys. Chem. C***112**2904

[3] Zhang T,Guo H and Qiao Y 2009 *J. Lumin.***129** 861

[4] Xie M-Y, Yu L, He H and Yu X-F 2009 *J. Solid State Chem.***182** (2009) 597

[5] Pedrinit C,Moinet B,Gacon JC andJacquier B 1992 *J.Phys.: Condens. Matter***4** 5461

[6] Liu Y, Chen W, Wang S, Joly AG, Westcott S and Woo BK 2008 *J. Appl. Phys.***103** 063105

[7] Yao M, Zhang X, Ma L, Chen W, Joly AG, Huang J and Wang Q 2010 *J. Appl. Phys.***108** 103104

[8] Wang Q, You Y, LudescherRD and Ju Y 2010 *J. Lumin.***130** 1076

[9] Zhu X, Zhang Q, Li Yand Wang H 2008 *J. Mater. Chem***18** 5060

[10] He H Xie MY Ding Y and Yu XT 2009 *Appl. Surface Scie.***255** 4623

[11] Yao M, Joly AG and Chen W 2010 *J. Phys. Chem. C***114** 826

[12] Inokuti M and Hirayama F 1965 *J. Chem. Phys.***43** 1978

[13] Vasquez SO 1999 *Physical Rev. B***60** 8575

[14] Walter JCG 1971 *Phys. Rev.* B **4** 648

[15] Dexter DL 1953 *J. Chem. Phys.***21** 836

[16] Scherrer P and Gottingen NGW 1918 *Math-Phys. Kl.***2** 96

[17] Carnall WT, Crosswhite H and Crosswhite HM 1978 Argonne National Laboratory Report ANL-78-XX-95

[18] Dorenbos P 2003 *J. Phys.: Condens. Matter***15** 6249

[19] Zheng J Guo Ca Ding X Ren Z and Bai J 2012 *Curr. Appl. Phys.***12** 643

[20] Wang Y Zhang J Hou D Liang H Dorenbos P Sun S and Tao Y 2012 *Opt.Mater.***34** 1214

[21] Wang B, Sun L andJu H 2010 *Solid State Comm.***150** 1460

[22] Fang Y-C, Huang X-R, Lin H-Y and Chu S-Y 2011 *J. Am. Ceram. Soc.***94**2735

[23] Solarz P and Romanowski WR 2007 *Radiat. Meas.***42** 759

[24] Nakazawa E and Shionoya S 1967 *J. Chem. Phys.***47** 3211